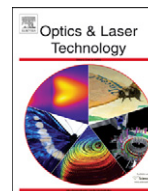




ELSEVIER

Contents lists available at [SciVerse ScienceDirect](http://www.sciencedirect.com)

## Optics &amp; Laser Technology

journal homepage: [www.elsevier.com/locate/optlastec](http://www.elsevier.com/locate/optlastec)

# Passively mode-locked erbium doped zirconia fiber laser using a nonlinear polarisation rotation technique

A. Hamzah<sup>a</sup>, M.C. Paul<sup>b</sup>, N.A. Awang<sup>c</sup>, H. Ahmad<sup>c</sup>, M. Pal<sup>b</sup>, S. Das<sup>b</sup>, M.A. Ismail<sup>a</sup>, S.W. Harun<sup>a,\*</sup>

<sup>a</sup> Department of Electrical Engineering, Faculty of Engineering, University of Malaya, 50603 Kuala Lumpur, Malaysia

<sup>b</sup> Fiber Optics and Photonics Division, Central Glass and Ceramic Research Institute, CSIR, Kolkata 70032, India

<sup>c</sup> Photonics Research Center, Department of Physics, University of Malaya 50603, Kuala Lumpur, Malaysia

## ARTICLE INFO

### Article history:

Received 17 November 2011

Received in revised form

7 August 2012

Accepted 13 August 2012

Available online 9 October 2012

### Keywords:

Passive mode locked fiber laser

Picosecond laser

Nonlinear polarization rotation

## ABSTRACT

A nonlinear polarization rotation (NPR) based mode-locked fiber laser is demonstrated using a 2 m long erbium-doped Zirconia–Yttria–Alumino Silicate fiber (EDZF) as the gain medium. The EDZF is drawn from a silica preform fabricated using the Modified Chemical Vapor Deposition (MCVD) method in which glass modifiers and nucleating agents are added using the solution doping technique. The fabricated EDZF has a core with dopant concentrations of 0.25 mol% of Al<sub>2</sub>O<sub>3</sub>, 2.10 mol% of ZrO<sub>2</sub> and 0.23 mol% of Er<sub>2</sub>O<sub>3</sub>, peak absorption of 22.0 dB/m at 978 nm and the fluorescence life-time of 10.86 ms. A stable picosecond laser is successfully obtained with pulse width of 0.32 ps and the repetition rate of 50 MHz using a simple ring cavity.

© 2012 Elsevier Ltd. All rights reserved.

## 1. Introduction

Recently, intensive research and development of Erbium doped fiber amplifiers (EDFAs) has spawned interest in other related areas including the various types of Erbium doped fiber lasers (EDFL) such as the mode-locked fiber lasers. For EDFAs, research efforts have focused on enhancing their performance, capability and compactness while reducing cost. In this regard, researchers are experimenting with new dopants such as alumina, phosphorus and new host materials such as telluride and bismuth [1–4]. The aim is to increase the erbium ion concentration in the fiber without incurring detrimental effects such as concentration quenching [5] and cluster formation [6]. However, these new materials are not without their drawbacks; Telluride and Bismuth based fibers cannot be easily spliced to conventional single-mode fibers (SMFs), thereby increasing the complexity of the amplifier and making it impractical for real-world applications. Hence, Zirconia has been seen as a highly promising candidate in the development of compact, high erbium concentration EDFAs [7,8]. Zirconia or ZrO<sub>2</sub> ions co-doped in silica fibers possess a high index of refraction of around 1.45 over the visible and near infrared spectrum. As such, ZrO<sub>2</sub> ions tend to exhibit wide emission and absorption bandwidths, as predicted by the Fuchtbauer–Ladenberg relationship [9,10] and Judd–Ofelt theory [11] and therefore can amplify more

wavelength division multiplexing (WDM) channels than lower index materials. Furthermore, zirconia has excellent mechanical strength and is chemically corrosion resistant as well as being non-hygroscopic, and is easily spliced to SMFs while exhibiting excellent transmission in the visible and near infrared giving the zirconia doped EDFA practical applications in the real world.

Nowadays, mode-locked fiber lasers are the corner-stone of ultrafast optics which have been used widely especially in medical and industrial applications [12,13]. There are two techniques to obtain mode-locked fiber laser; actively or passively. Active mode-locked fiber laser can be achieved using the periodic modulation of the resonator losses or using the round-trip phase change. In passive mode-locked fiber laser, an intensity fluctuation acts in conjunction with the fiber nonlinearity to modulate the cavity loss without external control. In this paper, the fabrication and characterization of an Erbium Doped Zirconia–Yttria–Alumino Silicate Fiber (EDZF) are demonstrated. Then, the mode-locked EDZF laser is presented using one of the passive mode-locked techniques called the nonlinear polarization rotation (NPR). The principle of the NPR technique relies on the Kerr effect in a length of optical fiber in conjunction with polarizers to introduce artificial saturable absorber action and achieve pulse shortening [14].

## 2. Fabrication of EDZF

The EDZF is fabricated in three stages; Modified Chemical Vapor Deposition (MCVD), solution doping and drawing processes. In the first stage, a conventional silica preform is fabricated using the

\* Corresponding author.

E-mail addresses: paulmukul@hotmail.com (M.C. Paul), swharun@um.edu.my (S.W. Harun).

MCVD technique, whereby  $\text{SiCl}_4$  and  $\text{POCl}_3$  vapors are passed through a slowly rotating silica tube that is heated by an external burner. The burner heats the length of the tube as it rotates and, due to the high temperature, the chloride of  $\text{SiCl}_4$  and  $\text{POCl}_3$  vapors oxidizes to deposit a porous phospho-silica layer along the inner wall of the silica tube. The optimum deposition temperature range for the MCVD process is 1350–1400 °C, with a variation of the pre-sintering temperature from 1300 to 1450 °C. The fabricated silica tube, with its deposited porous phospho-silica layer, then undergoes a solution doping process using dopant precursors of suitable strength to obtain the optimized process parameters for making a fiber with a numerical aperture (NA) of approximately 0.17–0.20. The glass modifiers,  $\text{ZrO}_2$ ,  $\text{Y}_2\text{O}_3$ ,  $\text{Al}_2\text{O}_3$  and  $\text{Er}_2\text{O}_3$  are incorporated individually into the host matrix from the oxidation process of soaked layer with an alcoholic and water mixture of ratio of 1:5 containing suitable strength of salt of  $\text{ZrOCl}_2 \cdot 8\text{H}_2\text{O}$ ,  $\text{YCl}_3 \cdot 6\text{H}_2\text{O}$ ,  $\text{AlCl}_3 \cdot 6\text{H}_2\text{O}$  and  $\text{ErCl}_3 \cdot 6\text{H}_2\text{O}$  respectively through the solution doping technique. Small quantities of  $\text{Y}_2\text{O}_3$  and  $\text{P}_2\text{O}_5$  are also added to the glass matrix to act as nucleating agents, functioning to increase the phase separation of the  $\text{Er}_2\text{O}_3$  doped micro-crystallites that will form in the core matrix of the optical fiber preform.

During the fabrication process, it is crucial to note that, in a bulk glass matrix, pure Zirconia exists in three distinct crystalline phases over different temperature ranges. At a very high temperature range, above 2350 °C,  $\text{ZrO}_2$  has a cubic structure—whereas, at intermediate temperature range between 1170 and 2350 °C, a tetragonal structure is observed. At low temperature range, below approximately 1170 °C,  $\text{ZrO}_2$  takes a monoclinic structure. The transformation of the crystalline structure from tetragonal to monoclinic is very rapid and is accompanied by a 3–5 percent volume increase. This rapid increase can result in extensive cracking in the material—as was observed in the doped core region of the preform after the fabrication—and is highly detrimental, as it destroys the mechanical properties of fabricated components during cooling. In order to overcome this problem, several oxides, such as  $\text{MgO}$ ,  $\text{CaO}$ , and  $\text{Y}_2\text{O}_3$  that dissolve in the Zirconia crystal structure can be used to slow down or eliminate these crystal structure changes; in this work a minute quantity of  $\text{Y}_2\text{O}_3$  is used.

In the final stage of the fiber fabrication process, the fabricated preform that has undergone the solution doping process is annealed at 1100 °C for 3 h in a closed furnace, under heating and cooling rates of 20 °C/min, to generate  $\text{Er}_2\text{O}_3$  doped  $\text{ZrO}_2$  rich micro-crystalline particles. The resulting annealed preform is drawn into a fiber strand with a diameter of  $125 \pm 0.5 \mu\text{m}$ , using a conventional fiber drawing tower. During the drawing process, the preform (and the fiber obtained) is exposed to a temperature of around 2000 °C for only a few minutes. Due to the high cooling rate of the material and the melting temperature of the  $\text{ZrO}_2$

crystals being above 2200 °C, the  $\text{ZrO}_2$  nano-crystalline host is retained within the silica glass matrix. Both the primary and secondary coatings are applied to increase the tensile strength, as well as to reduce the moisture ingress from external sources. During the fiber drawing procedure, proper control of the fiber diameter, coating thickness and coating concentricity along the whole length of the fabricated fiber gives the optimization required for the production of a high quality optical fiber. The thickness and uniformity of both coatings are ensured by adjusting the flow pressure of the inlet gases into the primary and secondary coating resin vessels—during the drawing of the fiber, as well as by properly aligning the position of the primary and secondary coating cup units.

In this work an EDZF which contains 0.25 mol% of  $\text{Al}_2\text{O}_3$ , 2.10 mol% of  $\text{ZrO}_2$  and 0.23 mol% of  $\text{Er}_2\text{O}_3$  dopant concentrations was fabricated. The core of the fiber has a diameter of 10  $\mu\text{m}$  with compositions of  $\text{SiO} + \text{Al}_2\text{O}_3 + \text{P}_2\text{O}_5 - \text{ZrO}_2 - \text{Y}_2\text{O}_3 + \text{Er}_2\text{O}_3$ . The fabricated fiber has an NA of 0.20, effective area of 75  $\mu^2$  and core refractive index of 1.47. Fig. 1 shows the spectroscopic properties of the fabricated fiber; spectral attenuation and fluorescence decay curves. As shown in Fig. 1(a), the peak absorption of the fiber is measured to be 22.0 dB/m at 978 nm. The fluorescence life-time of the fiber is 10.86 ms as shown in Fig. 1(b).

### 3. Configuration of the mode-locked EDZF laser

Fig. 2 shows the experimental setup for a passively mode-locked EDZF laser, which is based on NPR. The principle of an NPR technique relies on the Kerr effect in a length of an optical fiber

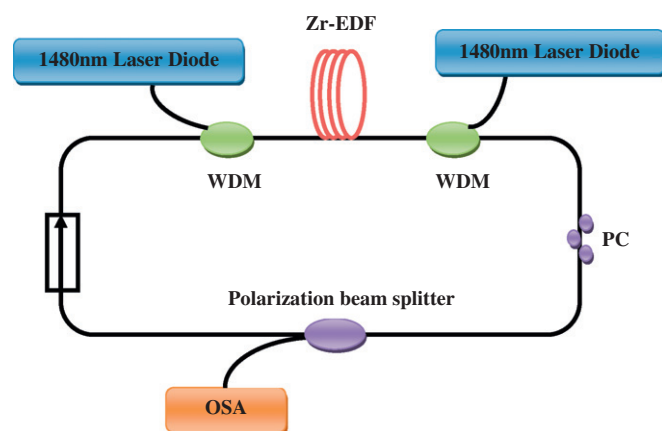


Fig. 2. Experiment setup for the proposed mode-locked EDZF laser.

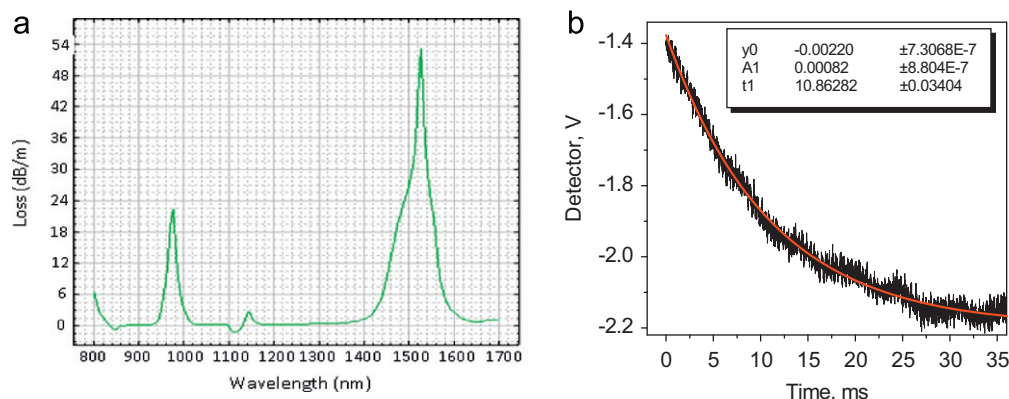


Fig. 1. Spectroscopic properties of the fabricated fiber (a) spectral attenuation and (b) fluorescence decay curves.

in conjunction with polarizers to introduce artificial saturable absorber action and achieve pulse shortening. The resonator consists of a piece of EDZF, 1480/1550 nm wavelength division multiplexer (WDM), polarization controller (PC), isolator and polarization beam splitter. The bi-directional 1480/1550 nm pumps are fixed at maximum pump power of 125 mW to provide amplification in both C- and L- band regions. The ring cavity consists of a 2 m long EDZF and a 2 m long standard single mode fiber (SMF-28) with a dispersion coefficient of 17 ps/nm km at  $\lambda = 1545$  nm which is inclusive of 1480 nm WDM, PC, isolator and coupler. The chromatic dispersion of the EDZF is experimentally determined to be 25.0 ps/nm km at 1550 nm. The fiber's zero chromatic dispersion wavelength is near 1.3  $\mu\text{m}$ , being similar to conventional telecommunication fibers widely used in practice, which makes it a good choice for the nonlinear-optics applications as well as mode-locked fiber laser. The PC is used to rotate the polarization state and allows a continuous adjustment of the birefringence within the cavity to balance the gain and loss for laser pulse generation. A standard optical isolator is used to ensure a unidirectional operation and acts as a polarizer. The laser power is coupled out using a polarization beam splitter which keeps 50% of the power inside the cavity. The spectral and temporal characteristics of the output laser are characterized using an optical spectrum analyzer (OSA) and an autocorrelator, respectively. The total cavity length 4 m and the total dispersion and the fundamental frequency are calculated to be  $0.084 \text{ ps nm}^{-1}$  and 50 MHz respectively.

NPR can be achieved when a linearly polarized light is incident on a piece of weakly birefringent fiber such as EDZF, and the polarization on the light will generally become elliptically polarized in this fiber. The elliptically polarized light can be considered as the superposition of two orthogonal linear polarization modes with different intensity, which experiences different nonlinear phase shifts as they propagate in the single-mode fiber due to the Kerr effect. This will result in a rotation of the light in the fiber whereby the orientation of the final light polarization is fully determined by the fiber length and its birefringence. The angle of rotation also correlates with the light intensity. If a polarizer (or polarization beam splitter) is put behind the fiber, the light intensity transmission through the polarizer will become light intensity dependent. With a proper selection of the orientation of the PC and the length of the fiber, an artificial saturable absorber could be achieved where light of higher intensity experiences less absorption loss on the polarizer. The proposed laser used this artificial absorption to achieve mode-locked fiber laser

and the nonlinearity of the fiber further shapes the pulse into the ultrashort pulse. The entire experimental setup is fusion-spliced together. Fig. 3 shows the output spectrum of the mode-locked EDZF laser showing a peak wavelength at 1563 nm. Kelly sidebands are also observed to indicate the stability of the pulse. These sidebands are a kind of resonant coupling, which occurs when some optical frequencies, the relative phase of soliton and dispersive wave changes by an integer of  $2\pi$  per resonator round trip. The small Kelly sidebands obtained suggest that the pulse duration is not the minimum possible value.

Fig. 4 shows the pulse train of the passive mode-locked laser obtained by tuning the polarization. The mode-locked pulse train exhibits enhancement compared to that of the Q-switching mode which is observed by an oscilloscope as an unstable pulse train with periodic variation in pulse amplitude. As evident in Fig. 4, the mode-locked pulse train has a constant spacing of 20 ns which translates to a repetition rate of 50 MHz. Fig. 5 shows the autocorrelator trace of the pulse, which shows the  $\text{sech}^2$  pulse profile with a full width half maximum (FWHM) of 0.32 ps. The center of the peaks is slightly offset from zero due to the instrument error. The experimental trace also shows two peaks in between the central peak which indicates that the pulse train is composed of a train of bound state of two pulses [15,16]. The output of the picoseconds is observed to be very stable at room temperature. The operation of the mode-locked fiber can be tuned by incorporating a tunable band-pass filter in the ring cavity. By optimizing the length of the EDZF, a wide-band tunable operation is also expected to be achieved up to the L-band region.

#### 4. Conclusion

A mode-locked fiber laser is successfully demonstrated using a 2 m long EDZF as the gain medium in conjunction with an NPR technique. The EDZF used is drawn from a silica preform fabricated using the MCVD method in conjunction with the solution doping process. The fabricated EDZF has a core dopant concentrations of 0.25 mol% of  $\text{Al}_2\text{O}_3$ , 2.10 mol% of  $\text{ZrO}_2$  and 0.23 mol% of  $\text{Er}_2\text{O}_3$  with peak absorption of 22.0 dB/m at 978 nm and the fluorescence life-time of 10.86 ms. The proposed laser is obtained using a simple ring cavity that generates a picosecond pulse with a pulse width of 0.32 ps and the repetition rate of 50 MHz.

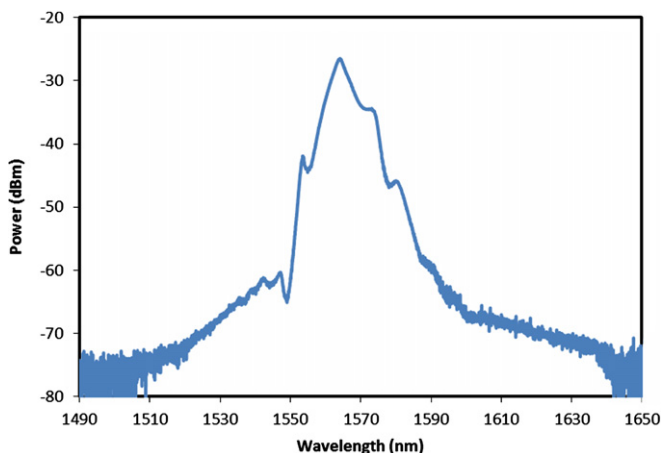


Fig. 3. Optical spectrum of the mode-locked EDZF laser.

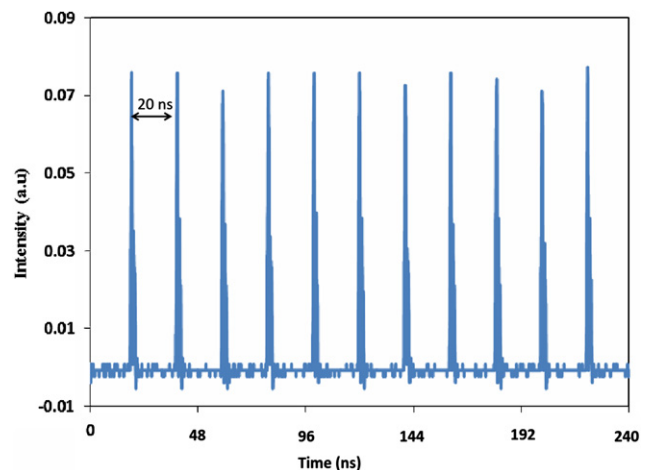


Fig. 4. Pulse train of the passive mode-locked laser with a repetition rate of 50 MHz.

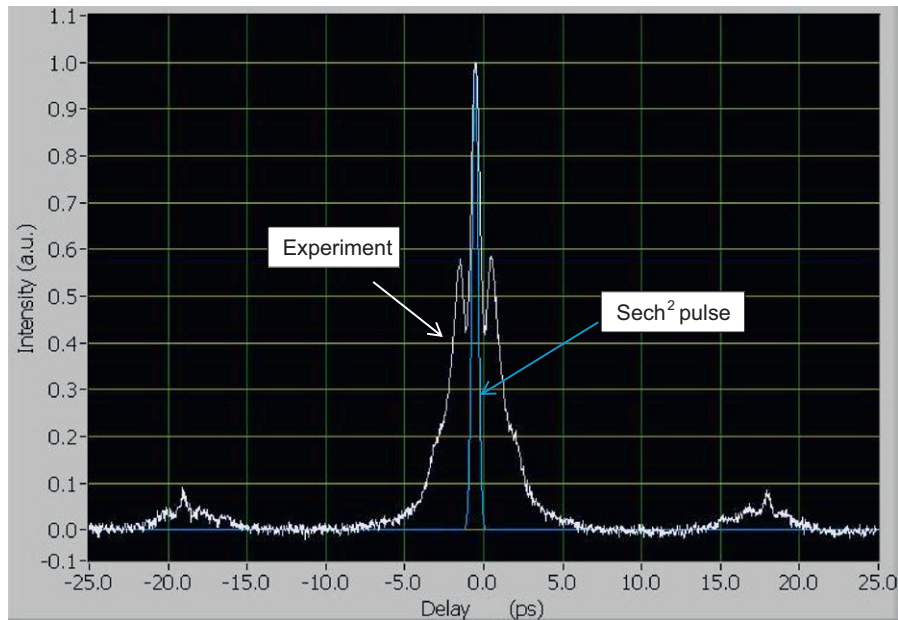


Fig. 5. Auto-correlator pulse trace with FWHM of 0.32 ps and Sech<sup>2</sup> pulse shape.

## References

- [1] Cucinotta A, Poli F, Selleri S. Design of erbium doped triangular photonic-crystal-fiber-based amplifiers. *IEEE Photonic Technology Letters* 2004;16(9): 2027–9.
- [2] Jiang S, Hwang BC, Luo T, Seneschal K, Smektala F, Honkanen S, Lucas J, Peyghambarian N. Net gain of 15.5 dB from a 5.1 cm-long Er<sup>3+</sup>-doped phosphate glass fiber. *Optical Fiber Communications Conference Proceedings*; 2000, PD5-1.
- [3] Ohishi Y, Mori A, Yamada M, Ono H, Nishida Y, Oikawa K. Gain characteristics of telluride-based erbium-doped fiber amplifiers for 1.5- $\mu$ m broadband amplification. *Optics Letters* 1998;23(4):246–74.
- [4] Cheng XS, Parvizi R, Ahmad H, Harun SW. Wide-Band bismuth-based erbium-doped fiber amplifier with a flat-gain characteristic. *Photonics Journal* 2009;1(5):259–64.
- [5] Snoeks E, Kik PG, Polman A. Concentration quenching in erbium-implanted alkali-silicate glasses. *Optical Materials* 1996;5:159–67.
- [6] Gill DM, McCaughan L, Wright JC. Spectroscopic site determinations in erbium-doped lithium niobate. *Physical Review B* 1996;53:2334–44.
- [7] Paul MC, Harun SW, Huri NAD, Hamzah A, Das S, Pal M, et al. Wideband EDFA based on erbium doped crystalline zirconia yttria alumino silicate fiber. *Journal of Lightwave Technology* 2010;28(20):2914–9.
- [8] Harun SW, Paul MC, Huri NAD, Hamzah A, Das S, Pal M, et al. Double-pass erbium-doped zirconia fiber amplifier for wide-band and flat-gain operations. *Optics and Laser Technology* 2011;43(7):1279–81.
- [9] Mahran O. Yttria–alumina–silicate erbium doped fiber amplifier characteristics at 1540 nm. *International Journal of Pure and Applied Physics* 2007;3: 83–90.
- [10] Liu G, Jacquier B. *Spectroscopic Property of Rare Earths in Optical Materials*. Heidelberg, Germany: Springer; 2005.
- [11] Walsh B. *Judd-Ofelt Theory: Principles and Practices*, *Advances in Spectroscopy for Lasers and Sensing*, vol. 33. The Netherlands: Springer; 2006 pp. 403–433.
- [12] Huan X, Ga F, Tama HY, Wai PKA. Stable and uniform multiwavelength erbium doped fiber laser using nonlinear polarization rotation. *Optics Express* 2006;14:8205–10.
- [13] Harun SW, Akbari R, Arof H, Ahmad H. Mode-locked bismuth-based erbium-doped fiber laser with stable and clean femtosecond pulses output. *Laser Physics Letters* 2011;8:449–52.
- [14] Nelson LE, Jones DJ, Tamura K, Haus HA, Ippen EP. Ultrashort-pulse fiber ring lasers. *Applied Physics B* 1997;65:277–94.
- [15] Amrani F, Niang A, Salhi M, Komarov A, Leblond H, Sanchez F. Passive harmonic mode locking of soliton crystals, *Optics Letter*, 36, 4239–41.
- [16] Zhao B, Tang DY, Shum P, Guo X, Lu C, Tam HY. Bound twin-pulse solitons in a fiber ring laser, *Physics Review E*, 70, 067602.